heme[25] is 2×10^5 s^{-1}. However, as in the cobalt case, one expects the corresponding rate constant for a hexacoordinate analogue to be several orders of magnitude faster[33] owing to the destabilizing effect of the electron in d_{z^2}.

The very weak bonds suggested for the photoactive state are a necessary condition for photochemical lability. It is important to recognize that *no* significant quantum yield is possible for a dissociative process from a thexi state with a subnanosecond lifetime *unless* the bonds are weak.

Bonding Effects in the Excited State. We have already seen in Table VI that ratios of excited-state rate constants *within a given complex* parallel ground-state values. However, there is no direct relationship between thermal lability and quantum yields *in different complexes*. For example CO is more labile than PBu_3 in $Fe(NPQH)_2(MeIm)(X)$ and has a ground-state activation enthalpy 7 kcal/mol smaller, yet the ϕ^N_{-CO} is 10^3 times greater than ϕ^N_{-P}. Generally π-acceptor ligands show substantially greater photolability than strictly sigma bonding ligands. The observation is not limited to CO. Quantum yields for PBu_3 vs. $P(OBu)_3$ also indicate that the better π-acceptor typically has a higher quantum yield even though ground state rates show $k^N_{-P} < k^N_{-PO}$. These observations suggest than π-bonding is less important in the excited state.

An angular overlap model[22] has been applied to the prediction of photochemical reactivity in coordination complexes. This model uses ground-state ϵ_σ and ϵ_π parameters to evaluate d orbital contributions to metal–ligand bonding in the excited state. These parameters are not available for the systems described here, nor are they likely to be useful. It is noted that spectroscopic parameters are very poor indicators even of ground-state bond strengths. We suggest that bond lengthening in the excited state will dramatically alter these ϵ_σ and ϵ_π parameters. For example, in a series of sterically hindered nickel complexes, ϵ_σ decreases by a factor of 2 for a 0.2 Å increase in Ni–N bond length.[35]

One expects π bonding to decrease even more in the excited state because of the more rapid decrease of π overlap with distance. This may explain the apparent contradiction that an excited state which is primarily σ^* results in the greatest labilization of π-acceptor ligands.

Perhaps also related to the diminished importance of π bonding in the excited state are the observations for DMGH in Table IV of a very small dependence of ϕ_{-N} on the trans ligand. In thermal reactions 10^4 k^T_{-N} values at 60°C are 158, 5.7, and 0.1 for T = PBu_3, $P(OBu)_3$, and BzNC, respectively, while 10^3 ϕ^T_{-N} values are 5, 6, and 3, respectively. We have previously proposed that the large trans delabilizing effects of π-acid ligands is due to the loss of synergistic π bonding in the transition state. In the photochemical process, most of the π bonding would already be lost in the photoactive state prior to ligand dissociation.

Summary

In summary, the following points are emphasized.

1. Thermal and photochemical axial ligand substitution in FeN_4XY systems both occur via a dissociative mechanism.
2. The temperature dependence of ϕ indicates that the potential well for the excited state of these complexes is well-defined and ϕ_{-X} is primarily dependent on the bond strength in the excited state.
3. Rate constant ratios for loss of X vs. Y in the excited state can be unequivocally established in these systems for a wide range of ligands.
4. The high quantum yields for CO photodissociation is attributed to a dramatically diminished importance of π bonding in the axially elongated excited state, which results in very weak metal–CO bonding.
5. A common photoactive state of picosecond lifetime involving d_{z^2} population is likely responsible for the gross similarities in photolability in a variety of FeN_4XY systems, including hemes, independent of the nature of the initial excitation. This state should parallel the ligation characteristics of the analogous cobalt (II) complex.

Acknowledgment. This work is supported by the Natural Sciences and Engineering Research Council of Canada.

Registry No. $Fe(DMGH)(MeIm)_2$, 57804-36-1; $Fe(DMGH)(MeIm)(PBu_3)$, 100485-22-1; $Fe(DMGH)(MeIm)(P(OBu)_3)$, 100485-23-2; Fe(DMGH)(MeIm)(BzNC), 59575-74-5; Fe(DMGH)(MeIm)CO, 61395-33-3; $Fe(DMGH)(PBu_3)_2$, 100485-25-4; $Fe(DMGH)(PBu_3)(P(OBu)_3)$, 100485-26-5; $Fe(DMGH)(PBu_3)CO$, 100485-29-8; $Fe(DMGH)(P(OBu)_3)_2$, 100485-30-1; $Fe(DMGH)(P(OBu)_3)CO$, 100485-33-4; $Fe(DMGH)(BzNC)_2$, 59575-75-6; $Fe(NPQH)(MeIm)_2$, 101915-88-2; $Fe(NPQH)(MeIm)(PBu_3)$, 101915-94-0; $Fe(NPQH)(MeIm)(P(OBu)_3)$, 101915-95-1; Fe(NPQH)(MeIm)(BzNC), 101915-92-8; Fe(NPQH)(MeIm)CO, 101915-97-3; $Fe(NPQH)(PBu_3)$, 101915-90-6; $Fe(NPQH)(PBu_3)(P(OBu)_3)$, 101915-98-4; $Fe(NPQH)(PBu_3)CO$, 101916-00-1; $Fe(NPQH)(P(OBu)_3)_2$, 101915-91-7; $Fe(NPQH)(P(OBu)_3)CO$, 101916-02-3; $Fe(NPQH)(BzNC)_2$, 101915-96-2.

Contribution from the Department of General and Inorganic Chemistry, Aristotelian University, Thessaloniki 54006, Greece

Electronic Ground States, Chemical Reactivity, and Related Properties of Square-Planar Platinum(II) Dithio Complexes

Evangelos G. Bakalbassis, George A. Katsoulos, and Constantinos A. Tsipis*

Received August 4, 1986

EHMO-SCCC calculations have been used in the analysis of the electronic structure, chemical reactivity, and related properties of four model platinum(II) complexes representing the set of compounds formed in the reactions of planar d^8 bis(1,1-dithiolato)platinum(II) complexes with phosphine bases. From the calculated molecular orbital description of the complexes and the frontier molecular orbital approach of chemical reactivity, plausible mechanisms of their formation reactions and fluxional behavior have been deduced. According to these mechanisms a frontier-controlled nonrigid quasi-five-coordinated four-center transition state is formed via a direct nucleophilic attack of the coordinated bidentate dithio ligand by the phosphine nucleophile. The role of sulfur and/or phosphorus 3d functions on the chemical bonding and reactivity of the complexes is also discussed. Overlap populations, two-center energy terms, and computed atomic charges of the complexes, compared to those of the corresponding free of metal ligand systems, were found to provide adequate information on the mechanism of the charge-transfer interactions involved in the bonding of the complexes.

Introduction

The interaction of Lewis bases with nickel triad dithiolates is a topic of considerable interest,[1-4] a variety of species being isolated, several of which have been structurally characterized. In particular, the reaction of phosphine bases with square-planar d^8

* To whom correspondence should be addressed.

(1) Coucouvanis, D. *Prog. Inorg. Chem.* **1979**, *26*, 301 and references cited therein; **1970**, *11*, 234.
(2) Burns, R. P.; McCullough, F. P.; McAuliffe, C. A. *Adv. Inorg. Chem. Radiochem.* **1980**, *23*, 211.

0020-1669/87/1326-3151$01.50/0

bis(1,1-dithiolato)metal(II) complexes, $M(S\text{-}S)_2$ [M = Pt or Pd; $(S\text{-}S)^- = R_2NCS_2^-$, $ROCS_2^-$, $(RO)_2PS_2^-$, and $R_2PS_2^-$], occurs by stepwise cleavage of metal–sulfur bonds to generate the four-coordinate square-planar $M(S\text{-}S)_2(PR'_3)$ and $[M(S\text{-}S)(PR'_3)_2]^+(S\text{-}S)^-$ complexes, which exhibit unidentate/bidentate and bidentate/ionic bonding modes of the 1,1-dithiolato groups, respectively.[5-14] Moreover, the corresponding bis(N-monosubstituted dithiocarbamato)metal(II) complexes react in a similar way but, in the presence of an excess phosphine, easily afford neutral dithiocarbimato complexes, $M(S_2C{=}NR)(PR'_3)_2$, via a deprotonation reaction on the coordinated bidentate dithio ligand.[15-19] In this respect the chemical behavior of the *N*-alkyldithiocarbamato ligands is similar to that of the isoelectronic xanthates, which easily undergo dealkylation reactions.[6,11] However, although important relationships between the solid-state and solution structures of several $M(S\text{-}S)_2$ complexes and their phosphine adducts have been established,[3,7] no answer to the question how and why phosphine nucleophiles substitutes for one of the two sulfur atoms that form a bidentate chelated ligand has yet been given. Therefore, we thought it would be advisable to direct our efforts toward understanding the mechanism of the aforesaid nucleophilic substitution reactions of square-planar platinum(II) and palladium(II) dithiocarbamates on the grounds of a theoretical approach based on quantum chemical calculations. In the study reported herein we have utilized the EHMO–SCCC method, in relation to the frontier molecular orbital theory of chemical reactivity, to investigate further the reactions of (dithiocarbamato)platinum(II) complexes with tertiary phosphine bases. The molecular orbital calculations were carried out on four model Pt(II) complexes, namely $Pt(S_2CNHR)_2$, $Pt(S_2CNHR)_2(PR'_3)$, $[Pt(S_2CNHR)(PR'_3)_2]^+$, and $Pt(S_2C{=}NR)(PR'_3)_2$, comprising the set of compounds involved in the nucleophilic substitution reactions studied. Particular emphasis has also been placed upon the interpretation of the observed electronic properties and chemical reactivities of these compounds with respect to their highly delocalized covalent bonding.

Computational Details

Calculations were carried out in the framework of the extended Hückel LCAO–MO method with self-consistent charge and configuration (EHMO–SCCC)[20,21] by using option 3 of the FORTICON-8 computer program.[22] In these iterative calculations the so-called "weighted H_{ij} formula" for the off-diagonal matrix elements (H_{ij}) was used in order to reduce the intriguing phenomenon of counterintuitive orbital mixing (COM) common in calculations of transition-metal complexes.[23]

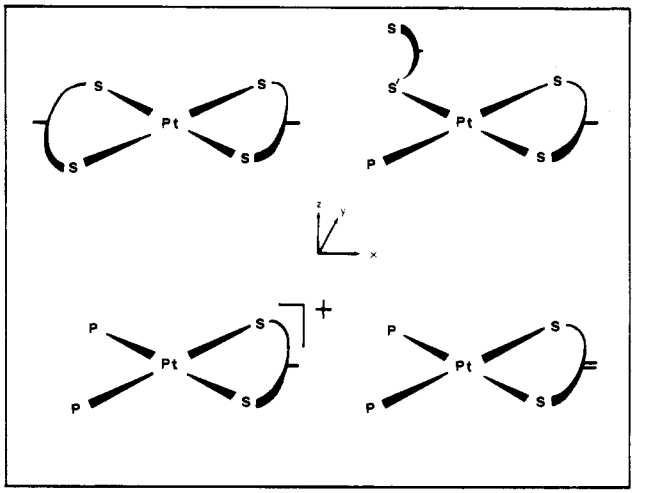

Figure 1. Molecular geometries of the compounds studied along with the coordinate system used.

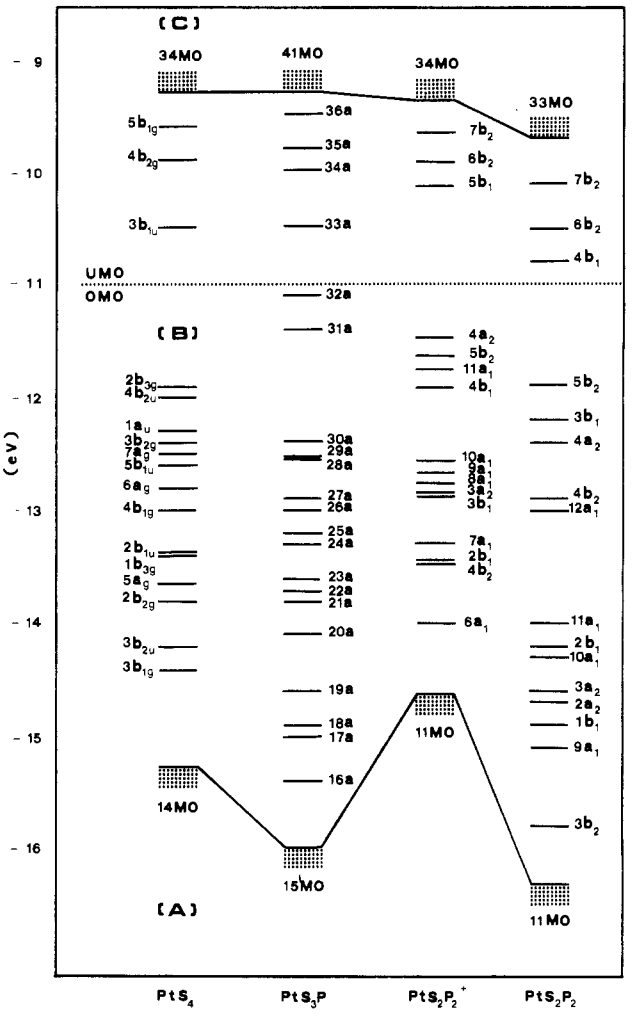

Figure 2. Electronic structure of the four model platinum(II) 1,1-dithiolates in their diamagnetic singlet ground state. For the sake of uniformity the eigenvalues of the $[PtS_2P_2]^+$ complex have been multiplied by 0.7.

(3) Fackler, J. P., Jr.; Thompson, L. D.; Lin, I. J. B.; Stephenson, T. A.; Gould, R. O.; Alison, J. M. C.; Fraser, A. J. F. *Inorg. Chem.* **1982**, *21*, 2397.
(4) Fackler, J. P., Jr.; Seidel, W. C.; Fetchin, J. A. *J. Am. Chem. Soc.* **1968**, *90*, 2707.
(5) Fackler, J. P., Jr.; Fetchin, J. A.; Seidel, W. C. *J. Am. Chem. Soc.* **1969**, *91*, 1217.
(6) Fackler, J. P., Jr.; Seidel, W. C. *Inorg. Chem.* **1969**, *8*, 1631.
(7) Lin, I. J. B.; Chen, H. W.; Fackler, J. P., Jr. *Inorg. Chem.* **1978**, *17*, 394.
(8) Stephenson, T. A.; Faithful, B. D. *J. Chem. Soc. A* **1970**, 1504.
(9) Alison, J. M. C.; Stephenson, T. A. *J. Chem. Soc. D* **1970**, 1092.
(10) Alison, J. M. C.; Stephenson, T. A.; Gould, R. O. *J. Chem. Soc. A* **1971**, 3690.
(11) Alison, J. M. C.; Stephenson, T. A. *J. Chem. Soc., Dalton Trans.* **1973**, 254.
(12) Steele, D. F.; Stephenson, T. A. *J. Chem. Soc., Dalton Trans.* **1973**, 2124.
(13) Tebbe, F. N.; Muetterties, E. L. *Inorg. Chem.* **1970**, *9*, 629.
(14) Cornock, M. C.; Gould, R. O.; Jones, C. L.; Owen, J. D.; Steele, D. F.; Stephenson, T. A. *J. Chem. Soc., Dalton Trans.* **1977**, 496.
(15) Katsoulos, G. A.; Manoussakis, G. E.; Tsipis, C. A. *Inorg. Chim. Acta* **1978**, *30*, L295.
(16) Katsoulos, G. A.; Tsipis, C. A. *Inorg. Chim. Acta* **1984**, *84*, 89.
(17) Katsoulos, G. A.; Manoussakis, G. E.; Tsipis, C. A. *Polyhedron* **1984**, *3*, 735.
(18) Tsipis, C. A.; Meleziadis, I. J.; Kessissoglou, D. P.; Katsoulos, G. A. *Inorg. Chim. Acta* **1984**, *90*, L19.
(19) Tsipis, C. A.; Kessissoglou, D. P.; Katsoulos, G. A. *Chem. Chron.* **1985**, *14*, 195.
(20) Hoffmann, R. *J. Chem. Phys.* **1963**, *39*, 1397.
(21) (a) Viste, A.; Gray, H. B. *Inorg. Chem.* **1964**, *3*, 1113. (b) Ballhausen, C. J.; Gray, H. B. *Inorg. Chem.* **1962**, *1*, 111.
(22) QCPE 344, FORTICON-8, Indiana University, Bloomington, IN.
(23) Ammeter, J. H.; Burgi, H. B.; Thibeault, J. C.; Hoffmann, R. J. *J. Am. Chem. Soc.* **1978**, *100*, 3686.

Table I. Eigenvalues and Character of the Valence MO's of Main Interest for the $Pt(S_2CNHR)_2$ Complex Exhibiting PtS_4 Coordination Geometry (D_{2h} Point Group)

MO	Γ_i[a]	MO type[b]	E_i, eV	charge distribn[c] Pt	4S	L	% S:|3d⟩
35	$5b_{1g}$	$S_4(\sigma$-LGO, xy, x, z^2, $y)$, $5d_{xy}$	−9.6 (−7.7)[d]	30	70	0	29
36	$4b_{2g}$	$S_4(\pi$-LGO, z, yz), $L(\pi)$, $5d_{xz}$	−9.9 (−8.9)	1	62	37	25
37	$3b_{1u}$	$S_4(\pi$-LGO, z, xz, $yz)$, $L(\pi)$, $6p_z$	−10.5 (−9.2)	3	58	39	37
38	$2b_{3g}$	$S_4(\pi$-LGO, z, yz, $xz)$, $5d_{yz}$	−11.9 (−11.3)	28	72	0	8
39	$4b_{2u}$	$S_4(\sigma$-LGO, y, x, x^2-y^2, $xy)$, $L(\sigma)$, $6p_y$	−12.0 (−12.0)	3	94	3	6
41	$3b_{2g}$	$5d_{xz}$, $L(\pi)$, $S_4(\pi$-LGO, z, $xz)$	−12.4 (−11.5)	52	23	25	5
42	$7a_g$	$5d_{z^2}/5d_{x^2-y^2}$, $S_4(\sigma$-LGO, y, x, $x^2-y^2)$	−12.5 (−11.6)	79	20	1	3
44	$6a_g$	$5d_{x^2-y^2}/5d_{z^2}$, $S_4(\sigma$-LGO, xy, s, x^2-y^2, $z^2)$	−12.8 (−11.7)	90	6	4	6
45	$4b_{1g}$	$S_4(\sigma$-LGO, y, s), $5d_{xy}$, $L(\sigma)$	−13.0 (−12.9)	18	68	14	0
47	$1b_{3g}$	$5d_{yz}$, $S_4(\pi$-LGO, z, xz, $yz)$	−13.4 (−12.9)	67	33	0	5
48	$5a_g$	$S_4(\sigma$-LGO, y, $x)$, $5d_{z^2}/5d_{x^2-y^2}$	−13.6 (−13.6)	29	71	0	0
49	$2b_{2g}$	$5d_{xz}$, $S_4(\pi$-LGO, z, yz, $xz)$, $L(\pi)$	−13.8 (−13.6)	39	38	23	4
51	$3b_{1g}$	$S_4(\sigma$-LGO, x, y, s), $5d_{xy}$, $L(\sigma)$	−14.4 (−14.2)	36	44	20	0

[a] The numbering scheme of the irreducible representation (Γ_i) of the MO wave functions corresponds to the valence-electron distribution; the HOMO and LUMO are the $2b_{3g}$ and $3b_{1u}$ MO's, respectively. [b] The basis functions in the particular eigenvector appear in decreasing order of their matrix elements, c_{ij} values; S_4 stands for the four sulfur donor atoms of the coordination sphere. [c] Percentage of the MO's total population located on the indicated atoms or group of atoms; L stands for all other ligand atoms not involved in the coordination sphere. [d] Figures in parentheses are the calculated values derived by neglecting the sulfur d AO's from the basis set.

Table II. Eigenvalues and Character of the Valence MO's of Main Interest for the $Pt(S_2CNHR)_2(PR'_3)$ Complex Exhibiting PtS_3P Coordination Geometry (C_1 Point Group)[e]

MO	Γ_i[a]	MO type[b]	E_i, eV	charge distribn[c] Pt	3S	P	L	% S, % P:|3d⟩
42	36a	$S_3(\sigma$-LGO, xy, $y)$, $P(x, y)$, $L(\sigma)$, $5d_{xy}/5d_{z^2}$	−9.5 (−5.4)[d]	6	57	15	22	42, 12
43	35a	$S_3(\sigma$-LGO, x, y, $xy)$, $P(xy, y, x)$, $5d_{xy}$, $L(\sigma)$	−9.8 (−7.8)	20	48	25	7	20, 15
44	34a	$P(z, z^2)$, $S_3(z, yz)$, $L(\pi)$, $5d_{xz}/5d_{yz}$	−10.0 (−8.0)	5	38	41	16	23, 25
45	33a	$S_3(\pi$-LGO, z, $xz)$, $L(\pi)$, $P(z, z^2)$, $6p_z/5d_{yz}$	−10.5 (−9.2)	5	43	17	35	25, 11
46	32a	L(s, z), $S_3(\sigma$-LGO, $xy)$, $5d_{xy}$	−11.1 (−9.9)	2	10	0	88	7, 0
47	31a	$L(\sigma)$, $S_3(\sigma$-LGO, x, y, $z)$, $5d_{x^2-y^2}$	−11.4 (−10.6)	4	37	2	57	4, 1
53	25a	$S_3(\pi$-LGO, z, $y)$, $5d_{xz}$, $L(\pi)$	−13.2 (−12.5)	32	38	3	27	2, 2
54	24a	$5d_{z^2}/5d_{xy}$, $S_3(\sigma$-LGO, x, $y)$, $L(\sigma)$	−13.3 (−12.6)	56	27	2	15	3, 0
55	23a	$5d_{z^2}/5d_{yz}$, $5d_{x^2-y^2}$, $S_3(\pi$-LGO, z, x, $y)$, $L(\pi)$	−13.6 (−12.9)	53	29	2	16	1, 1
56	22a	$5d_{x^2-y^2}/5d_{z^2}$, $S_3(\sigma$-LGO, x, $y)$, $L(\sigma)$, $P(x^2-y^2)$	−13.7 (−13.1)	69	21	4	6	3, 3
57	21a	$5d_{yz}/5d_{z^2}$, $S_3(\pi$-LGO, z, x, $y)$, $P(xz)$, $L(\pi)$	−13.8 (−13.5)	73	19	4	4	2, 3
58	20a	$5d_{xz}$, $S_3(\pi$-LGO, $z)$, $L(\pi)$	−14.1 (−13.9)	49	31	1	19	5, 1
60	18a	$L(\sigma)$, $S_3(\sigma$-LGO, x, y, $z)$, $5d_{xy}$	−14.9 (−14.2)	29	25	3	43	1, 0
61	17a	$L(\sigma)$, $S_3(\sigma$-LGO, y, $x)$, $5d_{xy}$	−15.0 (−14.7)	11	14	3	72	3, 0
62	16a	$S_3(\sigma$-LGO, y, s), $P(y, x)$, $L(\sigma)$, $5d_{xy}/5d_{x^2-y^2}$	−15.4 (−15.3)	16	30	28	26	2, 1

[a] See footnote *a*, Table I. [b] See footnote *b*, Table I. [c] See footnote *c*, Table I. [d] See footnote d, Table I. [e] The HOMO and LUMO are the 32a and 33a MO's, respectively; S_3 stands for the three sulfur donor atoms of the coordination sphere.

Moreover, a Madelung energy correction[22,24] was applied to the diagonal matrix elements, H_{ii}. The value of 1.65 was used for the parameter K, as this value was found by a series of calculations to give the best agreement between the experimental[16,17] and theoretical frequencies of the electronic transitions of the complexes studied.

Orbital exponents for sulfur, carbon, nitrogen, phosphorus, and hydrogen were those previously used.[22,25] Furthermore, the basis set of valence AO's for S and P consisted of 3s and 3p and/or 3s, 3p, and 3d functions with all being single Slater-type orbitals. The basis set of valence AO's for Pt consisted of 5d, 6s, and 6p with the last two being single Slater-type functions, whereas the 5d functions were considered as contracted linear combinations of two Slater-type functions. The exponents of the two d AO's were taken[22,26] as 6.013 and 2.696 with corresponding relative weights of 0.6333 and 0.5513. The 6s and 6p exponents for Pt were taken as 2.554 and 2.535, respectively.[27]

The geometries of the complexes were taken from the X-ray crystal data of the $Pt(S_2CNEt_2)_2$, $Pt(S_2CNH\text{-}t\text{-}Bu)_2(PCy_3)$, and $Pt(S_2C{=}NBz)(PEt_3)_2$ complexes.[28-30] For the sake of simplicity, as well as to avoid the use of very large basis sets, the alkyl substituents of the dithio and phosphine ligands were replaced by hydrogen atoms, the bond length values of P–H and N–H being 1.432 and 1.01 Å, respectively.[31] The molecular geometries of the compounds studied along with the coordinate system used are displayed in Figure 1.

Results and Discussion

Electronic Structure of Complexes. The electronic structure of the four model platinum(II) 1,1-dithiolates in their diamagnetic singlet ground state, based on the energy level diagram of the molecular orbitals (MO's) of main interest, is schematically depicted in Figure 2. From these data it seems that the eigenvalue spectrum of all four molecules could be divided into three distinct bands with respect to the nature of the MO's included. Band A in the region of −34.6 to −15.3 eV includes only pure ligand-bonding MO's, which do not affect the electronic properties and chemical reactivities of the compounds. The same also holds true for the MO's occurring in band C with an eigenvalue spectrum ranging from −9.3 to +72.2 eV. These MO's are mainly highly antibonding pure ligand and ligand–metal orbitals, with the latter involving only 6s and/or 6p metal component functions. Finally, band B in the region of −15.2 to −9.5 eV is the most important

(24) (a) Ohno, K. *Theor. Chim. Acta* **1964**, *86*, 1463. (b) Klopman, G. *J. Am. Chem. Soc.* **1964**, *86*, 1464, 4550.
(25) Ballhausen, C. J.; Gray, H. B. *Molecular Orbital Theory*; W. A. Benjamin: New York, 1964.
(26) (a) Richardson, J. W.; Nieuwpoort, W. C.; Powell, R. R.; Edgell, W. F. *J. Chem. Phys.* **1962**, *36*, 1057. (b) Richardson, J. W.; Powell, R. R.; Nieuwpoort, W. C. *Ibid.* **1963**, *38*, 796. (c) Clementi, E.; Raimondi, D. *Ibid.* **1963**, *38*, 2686.
(27) Basch, H.; Gray, H. B. *Theor. Chim. Acta* **1967**, *4*, 367.
(28) Amazov, A. Z.; Kuhina, G. A.; Porai-Koshits, M. A. *Zh. Struct. Khim.* **1967**, *8*, 174.
(29) Christides, P. C.; Rentzeperis, P. J. *Acta Crystallogr. Sect. B: Struct. Crystallogr. Cryst. Chem.* **1979**, *B35*, 2543.
(30) Schierl, R.; Nagel, U.; Beck, W. *Z. Naturforsch., B: Anorg. Chem., Org. Chem.* **1984**, *39B*, 649.
(31) *Interatomic Distances Supplements*; The Royal Society of Chemistry: London, 1965.

Table III. Eigenvalues and Character of the Valence MO's of Main Interest for the $[Pt(S_2CNHR)(PR'_3)_2]^+$ and $Pt(S_2C{=}NR)(PR'_3)_2$ Complexes Exhibiting PtS_2P_2 Coordination Geometries (C_{2v} Point Group)[e]

MO	Γ_i[a]	MO type[b]	E_i, eV	charge distribn[c] Pt	2S	2P	L	% S, % P:|3d⟩
		$[PtS_2P_2]^+$ Chromophore						
34	$8b_2$	$P_2(xz, z)$, $S_2(z, z^2)$, $L(\pi)$, $5d_{yz}$	−13.4 (−4.3)[d]	5	21	65	9	11, 40
36	$6b_2$	$P_2(z, xz)$, $S_2(x)$, $5d_{xy}$, $L(\pi)$	−14.1 (−11.8)	10	28	53	9	11, 27
37	$5b_1$	$S_2(z, xz)$, $L(\pi)$, $P_2(z, xz)$, $6p_z$	−14.5 (−13.1)	3	37	25	35	21, 15
38	$4a_2$	$S_2(z)$, $5d_{yz}$	−16.4 (−15.9)	5	95	0	0	6, 0
41	$4b_1$	$S_2(z)$, $L(\pi)$, $5d_{xz}$	−17.0 (−16.3)	13	49	2	36	1, 1
42	$10a_1$	$5d_{z^2}/5d_{x^2-y^2}$, $P_2(y, x)$, $S_2(x)$, $L(\sigma)$	−18.0 (−16.6)	88	3	6	3	0, 0
43	$9a_1$	$5d_{x^2-y^2}/5d_{z^2}$, $L(\sigma)$, $S_2(x)$, $P_2(x^2-y^2)$	−18.1 (−16.8)	69	12	5	14	2, 3
44	$8a_1$	$S_2(x)$, $L(\sigma)$, $5d_{x^2-y^2}$, $P_2(y, x)$	−18.2 (−16.9)	23	40	14	33	0, 4
45	$3a_2$	$5d_{yz}$, $S_2(z, x)$, $P_2(yz)$, $L(\pi)$	−18.3 (−17.0)	79	11	5	5	2, 3
46	$3b_1$	$5d_{xz}$, $L(\pi)$, $S_2(z, xz)$, $P_2(yz)$	−18.4 (−17.2)	75	9	2	14	2, 1
47	$7a_1$	$S_2(y)$, $L(\sigma)$, $5d_{x^2-y^2}$, $P_2(y)$	−19.0 (−17.8)	16	41	13	30	0, 4
48	$2b_1$	$L(\pi)$, $S_2(z)$, $5d_{xz}$	−19.2 (−18.1)	5	19	0	76	4, 0
49	$4b_2$	$5d_{xy}$, $P_2(y)$, $L(\sigma)$, $S_2(x)$	−19.3 (−18.6)	54	6	28	12	0, 0
		PtS_2P_2 Chromophore						
34	$7b_2$	$P_2(xy, x)$, $S_2(x)$, $5d_{xy}$, $L(\sigma)$	−10.1 (−7.7)	10	29	56	5	11, 38
35	$6b_2$	$P_2(xz, z)$, $S_2(y, xz)$, $L(\pi)$, $5d_{xy}$	−10.5 (−10.1)	8	16	65	11	9, 41
36	$4b_1$	$P_2(z, xz)$, $S_2(xz)$, $L(\pi)$, $6p_z/5d_{xz}$	−10.8 (−10.5)	9	13	66	12	7, 41
37	$5b_2$	$L(\sigma)$, $S_2(y)$, $P_2(y)$, $6p_y$	−11.9 (−11.7)	1	29	2	68	3, 1
39	$4a_2$	$S_2(z, yz)$, $5d_{yz}$, $L(\pi)$	−12.4 (−11.3)	4	92	1	3	6, 0
40	$4b_2$	$S_2(y)$, $L(\sigma)$, $P_2(y)$, $5d_{xy}$	−12.9 (−11.8)	10	58	11	21	5, 1
42	$11a_1$	$L(\sigma)$, $S_2(x, y)$, $5d_{x^2-y^2}/5d_{z^2}$, $P_2(y)$	−14.0 (−12.0)	25	30	5	40	3, 3
43	$2b_1$	$5d_{xz}$, $L(\pi)$, $S_2(z, y)$, $P_2(z, y)$	−14.2 (−12.4)	39	20	4	37	4, 2
44	$10a_1$	$5d_{z^2}/5d_{x^2-y^2}$, $S_2(x, y)$, $P_2(y)$	−14.3 (−12.5)	89	5	3	3	1, 1
45	$3a_2$	$5d_{yz}$, $S_2(x)$, $L(\sigma)$, $P_2(x)$	−14.6 (−12.9)	52	22	10	16	1, 5
46	$2a_2$	$5d_{yz}$, $S_2(z)$, $P_2(z)$, $L(\pi)$	−14.7 (−12.9)	66	16	9	9	1, 5
47	$1b_1$	$5d_{xz}$, $S_2(z)$, $L(\pi)$, $P_2(z)$	−14.9 (−13.3)	60	24	3	13	4, 2
48	$9a_1$	$5d_{x^2-y^2}$, $L(\sigma)$, $S_2(x, y)$, $P_2(y)$	−15.1 (−13.2)	33	26	9	32	1, 5
49	$3b_2$	$5d_{xy}$, $P_2(y, x)$, $L(\sigma)$, $S_2(x, y)$	−15.8 (−15.5)	57	4	33	6	0, 1

[a] See footnote *a*, Table I. [b] See footnote *b*, Table I. [c] See footnote *c*, Table I. [d] See footnote *d*, Table I. [e] The HOMO and LUMO of the $[PtS_2P_2]^+$ chromophore are the $4a_2$ and $5b_1$ MO's, respectively, whereas the corresponding ones of the PtS_2P_2 chromophore are the $5b_2$ and $4b_1$ MO's, respectively.

part of the energy level diagrams, including MO's mainly responsible for the chemical bonding and reactivity of the compounds. These MO's are highly mixed with substantial metal and ligand character. Consequently, it should be noted that band B includes also some pure ligand orbitals, involved in the characteristic intraligand and charge-transfer electronic transitions, although they do not contribute to the chemical bonding.

The calculated eigenvalues, charge distributions and partial wave analyses of the molecular orbitals responsible for the chemical bonding and reactivity of the complexes are listed in Tables I–III. For all complexes the eigenvalues are compared with those calculated by neglecting the sulfur 3d AO's from the basis set functions. The eigenvalues of both occupied and virtual orbitals are generally lowered by the inclusion of the sulfur and/or phosphorus 3d AO's with the virtual ones being more affected. This could be expected since most of the occupied MO's have less than 8% sulfur and/or phosphorus 3d character, whereas the virtual MO's acquire greater 3d character.

A further insight of the results shown in Tables I–III clearly demonstrates the importance of interactions between the Pt 5d orbitals and the ligand group orbitals (LGO's) of appropriate symmetry. The major contribution to the σ-bonding of all square-planar chromophores, PtS_4, PtS_3P, $[PtS_2P_2]^+$, and PtS_2P_2, comes from the lower energy MO's exhibiting a significant metal 5d (d_{xy}, $d_{x^2-y^2}$, d_{z^2}, or their mixtures allowed by symmetry) character. These MO's possess the symmetry species A_{1g} and B_{1g} for the PtS_4 chromophore (D_{2h} point group), A for the PtS_3P chromophore (C_1 point group), and A_1 and B_1 for the $[PtS_2P_2]^+$ and PtS_2P_2 chromophores (C_{2v} point group). For the PtS_3P chromophore, which exhibits a very low symmetry, the expected mixing of the metal 5d functions allowed by symmetry is observed. Therefore, the $5d_{xz}$ and $5d_{yz}$ metal functions, involved in the π-bonding, are mixed with the $5d_{xy}$, $5d_{x^2-y^2}$, and $5d_{z^2}$ ones. Significant interactions between $5d_{xz}$ and $5d_{yz}$ and LGO's of π-type are also predicted for all four complexes. These π-MO's possess the symmetry species B_{2g} and B_{3g} for the PtS_4, A for the PtS_3P, and B_1 and A_2 for the $[PtS_2P_2]^+$ and PtS_2P_2 chromophores. It is also interesting to note that for all complexes the π-MO's with a strong $5d_{yz}$ character are mainly localized on the chelate rings, while those with a strong $5d_{xz}$ character have an appreciable localization on the substituents as well. Accordingly, the nature of the π-MO's strongly suggests a degree of cyclic electron delocalization on the four-membered chelate rings, as a result of the π-bonding effect. Data (Tables I–III) also indicate that the metal–ligand σ-coupling via $5d_{xy}$ exceeds the interaction via $5d_{z^2}$ and $5d_{x^2-y^2}$, whereas the contribution of the $5d_{xz}$ and $5d_{yz}$ AO's to the π-coupling is almost the same. This difference is rationalized on the basis of the Pt 5d populations shown in Table IV. Large Pt AO populations are predicted for $5d_{z^2}$, $5d_{x^2-y^2}$, $5d_{xz}$, and $5d_{yz}$ ($\sim$1.8–1.9 e), whereas the $5d_{xy}$ population is significantly reduced ($\sim$1.2–1.4 e). Furthermore, the very low AO population of the Pt $6p_x$, $6p_y$ ($\sim$0.2 e), and $6p_z$ ($\sim$0.02 e) orbitals clearly demonstrates that these AO's do not participate in the chemical bonding of all complexes. None of these AO's were found to contribute more than 3% to the formation of the bonding MO's of the complexes (Tables I–III). However, the Pt 6s AO has an

Table IV. Atomic Orbital Populations of the Central Atom of the PtS_4, PtS_3P, $[PtS_2P_2]^+$, and PtS_2P_2 Coordination Geometries

AO	orbital population PtS_4	PtS_3P	$[PtS_2P_2]^+$	PtS_2P_2
6s	0.524 (0.496)[a]	0.560 (0.516)	0.468 (0.439)	0.583 (0.507)
$6p_x$	0.170 (0.176)	0.210 (0.245)	0.158 (0.201)	0.248 (0.294)
$6p_y$	0.168 (0.287)	0.212 (0.294)	0.154 (0.238)	0.258 (0.340)
$6p_z$	0.012 (0.028)	0.018 (0.021)	0.002 (0.005)	0.045 (0.037)
$5d_{x^2-y^2}$	1.866 (1.994)	1.787 (1.977)	1.835 (1.962)	1.714 (1.957)
$5d_{z^2}$	1.901 (1.941)	1.916 (1.941)	1.901 (1.958)	1.932 (1.952)
$5d_{xy}$	1.157 (0.959)	1.280 (1.061)	1.355 (1.160)	1.370 (1.220)
$5d_{xz}$	1.837 (1.933)	1.836 (1.966)	1.873 (1.970)	1.814 (1.977)
$5d_{yz}$	1.882 (2.000)	1.845 (1.983)	1.864 (1.982)	1.812 (1.978)

[a] Figures in parentheses are the calculated values derived by neglecting the sulfur d AO's from the basis set.

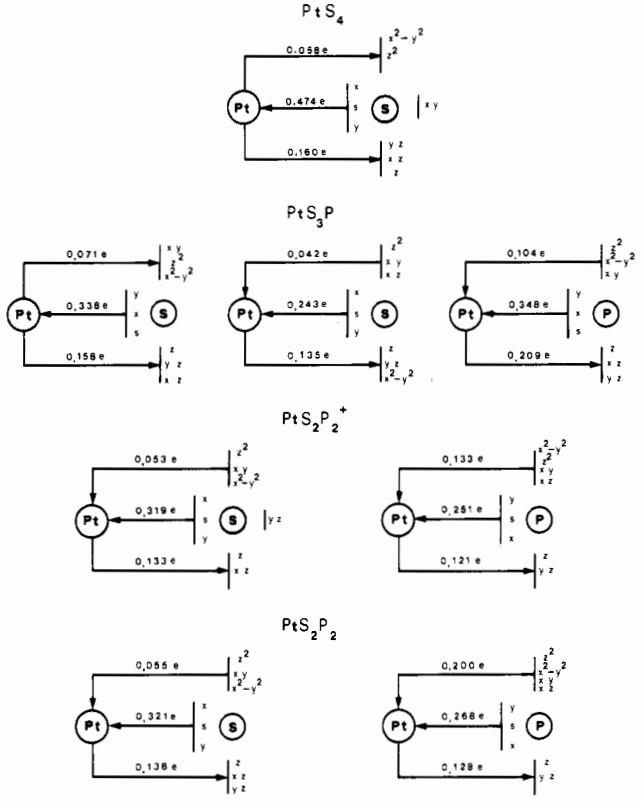

Figure 3. Charge-transfer interactions for the coordination bonds of the PtS_4, PtS_3P, $[PtS_2P_2]^+$, and PtS_2P_2 complexes.

appreciable contribution to the σ-bonding acquiring a total electron population of $\sim$0.5–0.6 e.

The inclusion of the sulfur 3d AO's in the basis set results in the increasing of the $5d_{xy}$ population and the concomitant decreasing of the $5d_{x^2-y^2}$, $5d_{xz}$ and $5d_{yz}$ populations, whereas those of the remaining AO's are less affected. This is a clear indication that the Pt $5d_{xy}$ AO is involved in charge-transfer (CT) interactions of the L $\rightarrow$ M type (LMCT) with the sulfur d functions, whereas the $5d_{x^2-y^2}$, $5d_{xz}$, and $5d_{yz}$ ones are involved in the corresponding MLCT interactions. In order to gain further insight on the nature of the CT interactions between the central metal atom and the ligands, the atomic orbital populations of the ligand donor atoms of the complexes were compared with those of $[(S_2CNHR)_2]^{2-}$, $[(S_2CNHR)_2(PR'_3)]^{2-}$, $[(S_2CNHR)(PR'_3)_2]^-$, and $[(S_2C{=}NR)(PR'_3)_2]^{2-}$ free of metal ligand systems. These results are presented in Table V[32] and schematically depicted in Figure 3.

Data in Figure 3 provide adequate information on the mechanism of the CT interactions occurring in all complexes and demonstrate the role of sulfur and phosphorus 3d functions on the chemical bonding of the compounds. The following general conclusions could be drawn:

Both LMCT and MLCT interactions occur in each coordination bond of all complexes. The sulfur and phosphorus s, p_x, and p_y AO's are involved only in the LMCT interactions, whereas the p_z, d_{xz}, and d_{yz} AO's are involved mainly in the MLCT ones (π-back-bonding). It is interesting to note that the π-back-bonding effect for the PtS_4 coordination geometry operates mainly via sulfur d_{yz} and d_{xz} AO's, whereas for the PtS_3P, $[PtS_2P_2]^+$, and PtS_2P_2 coordination geometries significant contribution results also from sulfur and phosphorus p_z AO's. The sulfur and phosphorus $d_{x^2-y^2}$, d_{z^2} and d_{xy} AO's contribution to the CT (L $\rightarrow$ M and/or M $\rightarrow$ L) interactions of all complexes seems less important, depending on the nature of the coordination bonds.

It is also obvious from Figure 3 that phosphorus is a better σ-donor than the sulfur donor atoms of the dithio ligands, their π-acceptor capacity being about the same. Therefore, the substitution of the sulfur by the stronger nucleophile phosphorus donor atom is now well understood. This was further supported on the basis of electronic criteria by performing calculations on the two hypothetical isoelectronic $Pt(S_2CNH_2)(SH_2)(SH)$ and $Pt(S_2CNH_2)(PH_3)(SH)$ complexes. Actually, it was found that the substitution of a sulfur by a phosphorus donor atom is energy favored by about 82 kcal·mol^{-1}. Furthermore, it should be noted that the sulfur atom of the unidentate dithioligand is a better σ-donor and π-acceptor atom than the sulfur atoms of the bidentate one.

(32) Supplementary material.

Table VI. Two-Center Energy Terms and Overlap Populations for the Coordination Bonds of the PtS_4, PtS_3P, $[PtS_2P_2]^+$, and PtS_2P_2 Coordination Geometries

chromophore	Pt–X[a]	energy, eV	overlap population
PtS_4	Pt–S	−4.3649	0.5193
PtS_3P	*trans*-Pt–S	−4.1264	0.4873
	cis-Pt–S	−4.3687	0.5072
	Pt–S′	−4.8155	0.5615
	Pt–P	−6.2743	0.7335
$[PtS_2P_2]^+$	Pt–S	−3.2532	0.4154
	Pt–P	−4.8052	0.5948
PtS_2P_2	Pt–S	−4.4435	0.5155
	Pt–P	−6.8461	0.7663

[a] S′ stands for the coordinated sulfur atom of the unidentate dithio ligand.

The above results are also consistent with the two-center energy terms and overlap population data for the coordination bonds of the compounds under investigation listed in Table VI. This could be expected assuming that both the two-center energy terms and overlap populations reflect the strength of the coordination bonds. According to these data the following sequence for the strength of coordination bonds is obtained:

$$\text{Pt–P} > \text{Pt–S}' > \text{Pt–S}$$

In addition, the Pt–S bonds of the dithiocarbimato ligand are predicted to be stronger than the Pt–S bonds of the dithiocarbamato one. Finally, it should be noted that the introduction of the phosphine molecule results in weakening of the *trans*-Pt–S bond of the bidentate dithioligand in the PtS_3P coordination geometry. This finding clearly demonstrates the trans influence or structural trans effect (STE) of the phosphine ligand.[33]

Ground-State Properties and Mechanisms. On the basis of the molecular orbital description of complexes and the frontier molecular orbital approach of chemical reactivity, a qualitative interpretation of their most important ground-state properties along with inferences about the mechanistic aspects of their chemical reactivities could be attempted.

First of all, it was verified experimentally[3,6,7,11] that none of the compounds reacting with Lewis bases, such as phosphines and amines, yield five- or six-coordinated adducts. This is not surprising if we take into account the character and energy of the frontier MO's. Actually, none of the LUMO's of the complexes exhibited appreciable character of metal AO functions in their axial positions, and this was also the case with their NLUMO's (Tables I–III). Therefore, a direct frontier controlled nucleophilic attack of the electrophilic central metal atom, resulting in the expansion of their coordination number, by axial σ-bonds formation, is not possible. Hence, the formation of five- and six-coordinated adducts seems very unlikely. Accordingly, on the basis of the fact that nucleophilic substitution reactions occur through frontier MO's interactions, a question immediately arises as to how phosphine nucleophiles substitute for one of the two sulfur donor atoms that form a bidentate chelated ligand.

It is well-known[34] that nucleophilic substitution reactions of square-planar Pt(II) complexes proceed via an S_N2 mechanism involving the formation of five-coordinated intermediates. Such a mechanism was also proposed for the reactions of platinum(II) 1,1-dithiolates with phosphine bases on the grounds of experimental

(33) Elder, R. C.; Heeg, M. J.; Payne, D.; Tricula, M.; Deutsch, E. *Inorg. Chem.* **1978**, *17*, 431.

(34) Tobe, M. L. *Inorganic Reaction Mechanisms*; Nelson: London, 1972.

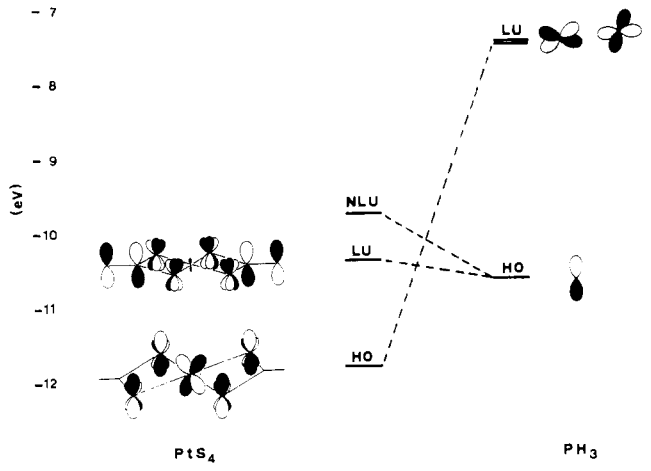

Figure 4. Frontier MO interactions between the PtS_4 complex and the phosphine nucleophile.

evidence.[3,4] It was also stated that five-coordinated adduct formation precedes ligand substitution. However, as was shown previously, the LUMO of PtS_4 coordination geometry is mainly localized on the π-system of the two dithiocarbamato ligands. This was in line with the inability of the complex to form adducts by trapping Lewis bases. Therefore, it seems very likely that the nucleophilic attack should occur on the coordinated ligand and not on the central atom itself. At first look, due to the high delocalizability of the LUMO on all four atoms of the S_2CN moiety, any one of these atoms could be the center for a nucleophilic attack. With this kept in mind, a variety of products could be formed, depending on both the nature of the particular nucleophile and the charge distribution on the four atoms. The driving force for the orientation of the particular nucleophile toward the S_2CN moiety arises mainly from both the optimization of the frontier MO's and electrostatic interactions between the electrophilic center and the nucleophile. For the neutral phosphine nucleophiles these interactions are mainly frontier controlled. Therefore, their optimization occurs by the orientation of the phosphine molecule over the two sulfur atoms of the S_2CN moiety, since this orientation provides the best LUMO, NLUMO–HOMO and HOMO–LUMO overlapping between the electrophile and nucleophile. These frontier MO's interactions are demonstrated schematically in Figure 4. It should be also noted that although the HOMO (electrophile)–LUMO (nucleophile) interaction was less favorable than the LUMO to NLUMO–HOMO one, due to the energy matching criterion, it plays an important role in the formation of the Pt–P bond. It is obvious then that the nucleophilic substitution of the one sulfur atom of the bidentate dithio ligand by the phosphine nucleophile proceeds through a four-center transition state, schematically depicted as in **1**. In this transition

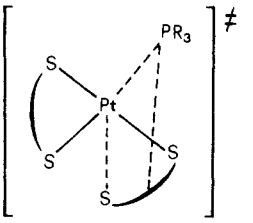

1

state, which could be considered as a quasi-five-coordinated intermediate, in line with experimental evidence reported earlier by Fackler et al.,[3,4] both the formation of Pt–P bonds and the weakening of Pt–S bonds were involved. Such a concerted mechanism, involving transition state **1**, is favored by the small negative entropy values reported previously.[12]

If the least-motion path for the attack of the phosphine molecule is applied along with the nature of the frontier MO's interactions, a trigonal-bipyramidal rather than a square-pyramidal configuration for the four-center transition state seems more possible. Furthermore, the frontier MO's interactions strongly suggest that the transition state is not a static one, but intramolecular rearrangements could also easily occur. Since the LUMO of PtS_4 complex is delocalized on both dithio ligands, the phosphine molecule could easily migrate from one ligand to the other in the transition state, probably through a square-pyramidal transition state (Berry pseudorotation mechanism). Therefore, a reasonable understanding of the formation mechanism of the PtS_3P complexes and their fluxional behavior, established experimentally by dynamic NMR data,[3,11] has now been confirmed. This mechanism is depicted schematically in Figure 5. Moreover, from the molecular orbital point of view, these intramolecular rearrangements involve interchanges between the HOMO and LUMO of the PtS_3P complex. Such interchanges are energy allowed due to the very low HOMO–LUMO energy gap (ca. 0.6 eV or $\sim$13.8 kcal·mol^{-1}) in the PtS_3P complexes. This energy gap is very close to the activation energy value derived from the NMR data for the intramolecular rearrangements in analogous PtS_3P complexes[3] (e.g. 12.4 kcal·mol^{-1} for the platinum(II) dithiophosphates).

The substitution of one more sulfur donor atom of the dithio ligands in PtS_3P complex by a second phosphine nucleophile is now considered. The LUMO of the PtS_3P complex is mainly localized on the π-system of the bidentate dithio ligand. Consequently, this ligand should be the center of a new nucleophilic attack by the second phosphine nucleophile. The frontier MO's

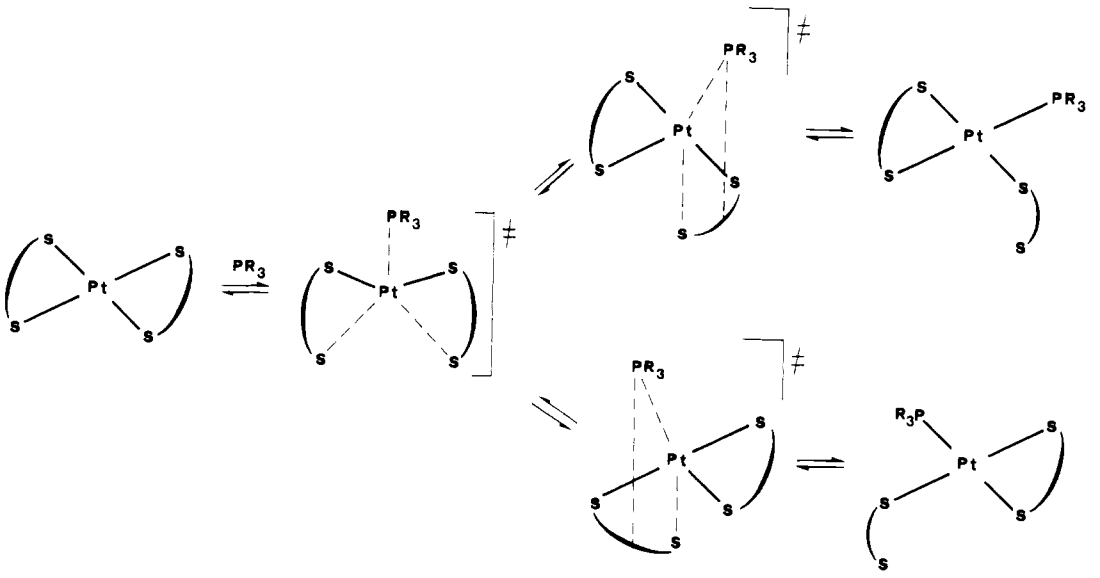

Figure 5. Proposed mechanism for the formation of PtS_3P coordination geometries and their fluxional behavior.

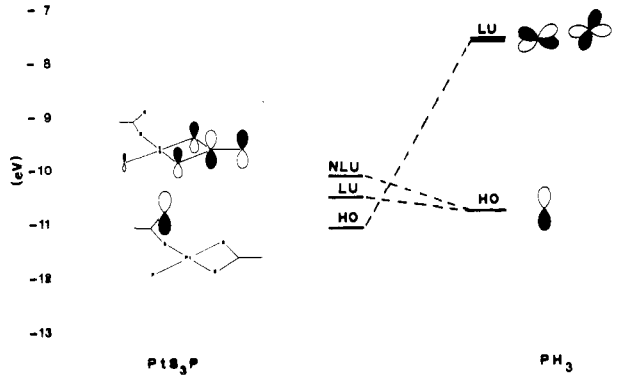

Figure 6. Frontier MO interactions between the PtS_3P complex and the phosphine nucleophile.

interactions responsible for the formation of the transition state are schematically shown in Figure 6. In a similar way, a quasi-five-coordinated nonrigid transition state exhibiting a trigonal-bipyramidal stereochemistry is formed. In this transition state several intramolecular rearrangements are possible, depending on the nature of the phosphine nucleophile and the dithio ligands, as well. The formation of the neutral *trans*-PtS_2P_2 coordination geometry with two dangling dithio ligands seems very probable, as a first step. This fluxional intermediate could be easily rearranged to yield the cationic $[PtS_2P_2]^+$ complex with a bidentate ligand and a noncoordinated thiolate anion. Phosphine exchange could also be possible. All these processes, depicted schematically in Figure 7, have been verified experimentally by dynamic NMR measurements,[3] as well. Furthermore, the anionic noncoordinated dithio ligand (nucleophile) could also attack again the cationic $[PtS_2P_2]^+$ complex, whose HOMO and LUMO are schematically depicted in **2** and **3**, respectively. However, in this case, due to the bad energy matching[16] of the frontier MO's interactions and the negative charge on the nucleophile, the nucleophilic attack must be predominantly electrostatically controlled. Therefore, the nucleophile will attack the electrophilic centers exhibiting positive net charges, i.e. the Pt(II) central atom (+0.39 e) or the hydrogen atom (+0.12 e) of the amine group of the dithio ligand. In the first case, the $[PtS_2P_2]^+$ complex will be converted into the PtS_3P complex, possibly via the neutral *trans*-PtS_2P_2 intermediate according to

$$[PtS_2P_2]^+ + S\text{–}S^- \rightleftharpoons [\textit{trans}\text{-}PtS_2P_2]^\ddagger \rightleftharpoons PtS_3P + P$$

The dependence of this equilibrium on the polarity of solvents used[7,10,11] strongly supports the predominantly electrostatic character of the direct nucleophilic attack of the central atom by the $S\text{–}S^-$ nucleophile. Such an electrostatically controlled direct nucleophilic attack of the central atom by the $S\text{–}S^-$ nucleophile also accounts well for the formation of $[PtS_6]^-$ complexes, assuming reaction of the PtS_4 complexes with an excess of dithio ligands.[14] In the second case, a deprotonation of the bidentate dithio ligand occurs, yielding the PtS_2P_2 complex, which possesses a bidentate dithiocarbimato ligand. It is expected that an excess of phosphine should favor this deprotonation reaction, possibly due to the blocking out of the electrophilic central atom via frontier MO's interactions. Hence, the hydrogen atom, being the only electrophilic center left, could be cleaved. Actually, this is the case for the deprotonation reactions reported previously.[16,18] Moreover, the frontier MO's interactions between an excess phosphine and the $[PtS_2P_2]^+$ complex easily explain the rapid phosphine exchange established by dynamic NMR data.[7] This process and the dithiolate exchange are favorable processes due to the weakening of both Pt–P and Pt–S bonds in the $[PtS_2P_2]^+$ coordination geometry (Table VI). Phosphine exchange is also predicted to occur in the dithiocarbimato complex PtS_2P_2 as its LUMO, schematically depicted in **4**, is mainly localized on the

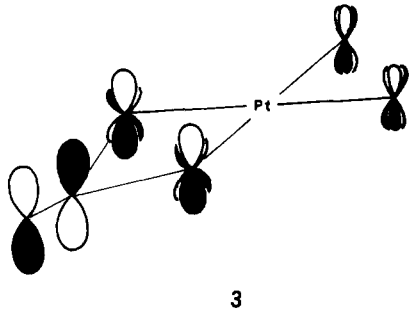

3

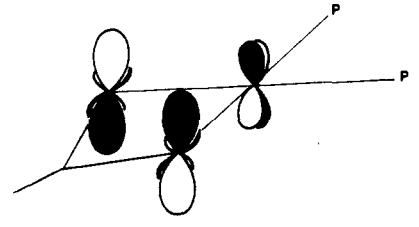

2

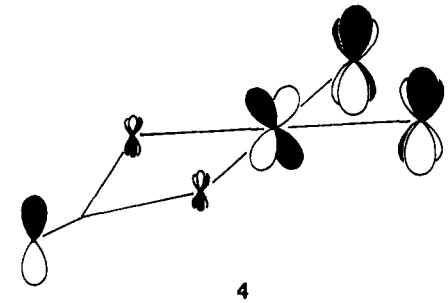

4

two phosphine ligands. It is interesting to note that, for the dithiocarbimato complex, its HOMO, **5**, is mainly localized on

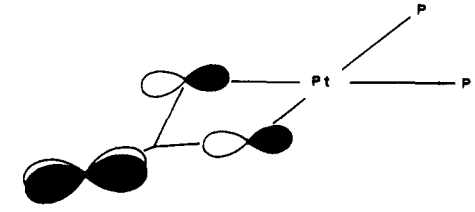

5

the nitrogen atom of the dithiocarbimato ligand. Therefore, this nitrogen atom should be the nucleophilic center of the complex

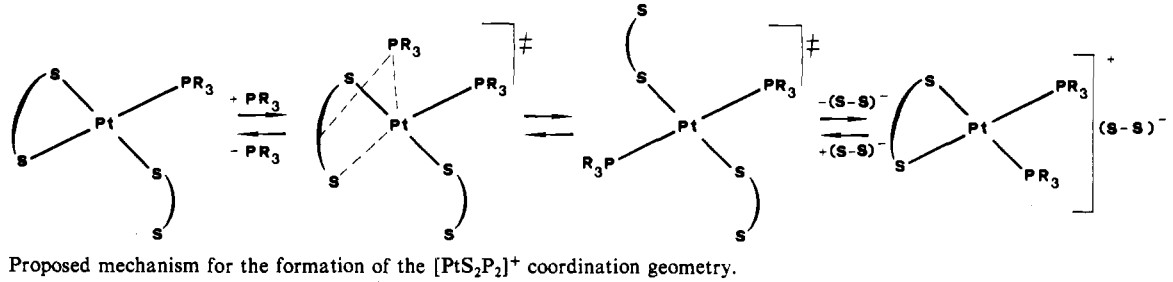

Figure 7. Proposed mechanism for the formation of the $[PtS_2P_2]^+$ coordination geometry.

in reactions with electrophiles. Actually, the dithiocarbimato complex reacts with the electrophile H^+, affording the protonated product on the nitrogen atom, namely the $[PtS_2P_2]^+$ complex.[16]

Registry No. $Pt(S_2CNHR)_2$ (R = H), 92272-20-3; $Pt(S_2CNHR)_2(PR'_3)$ (R = R' = H), 109687-54-9; $[Pt(S_2CNHR)(PR'_3)_2]^+$ (R = R' = H), 109687-55-0; $Pt(S_2C{=}NR)(PR'_3)_2$ (R = R' = H), 109687-53-8.

Supplementary Material Available: Table V, listing atomic orbital populations of the ligand donor atoms of PtS_4, PtS_3P, $[PtS_2P_2]^+$, and PtS_2P_2 (1 page). Ordering information is given on any current masthead page.

Contribution from the Department of Chemistry, University of Houston, Houston, Texas 77004, and Istituto per lo Studio della Stereochemica ed Energetica dei Composti di Coordinazione, ISSECC-CNR, 50132 Firenze, Italy

Rearrangements in ML_n Complexes of Diazenes and the Ligand-Substitution Reaction

Sung-Kwon Kang,[†] Thomas A. Albright,*[†] and Carlo Mealli[‡]

Received February 24, 1987

The rearrangement of a $Cr(CO)_5$ unit from one coordination site to another has been studied for *cis*- and *trans*-H_2N_2, pyridazine, naphthyridine, and phenanthroline complexes by means of extended Hückel calculations. The results for the 1,2-shift process in (*cis*-H_2N_2)$Cr(CO)_5$ were checked at the ab initio level and found to be in qualitative agreement with the extended Hückel calculations. In both isomers of H_2N_2 the favored reaction pathway is via a π-bonded species rather than a 20-electron complex (for the cis isomer) where the lone pairs on both nitrogens simultaneously interact with $Cr(CO)_5$. For pyridazine- and naphthyridine-$Cr(CO)_5$ the transition states are categorized by very long Cr-N distances; in other words, they contain substantial dissociative character. This study is extended to 16-electron square-planar analogues, namely pyridazine-, naphthyridine-, and phenanthroline-$PtCl_3^-$. The transition states in these cases are much more associative. Finally, a general analysis of ligand substitution at 18-electron complexes vs. nucleophilic substitution reactions in saturated, 8-electron compounds is developed. This analysis shows that ligand-substitution reactions at 18-electron ML_n complexes, where L is a strong σ donor, are unlikely to proceed via an S_N2 transition state. This is entirely consistent with the numerical results for the diazene-$Cr(CO)_5$ complexes. In general a strong antibonding interaction between a filled metal d orbital and incoming ligand lone pair is turned on. In contrast, for organic/main group compound nucleophilic substitution reactions an S_N2 pathway is viable. The nucleophile lone-pair orbital evolves into a nonbonding orbital.

Introduction

The ligand-substitution reaction is probably the most important fundamental step in organometallic reaction mechanisms. The vast majority of proposed mechanisms require at least one ligand-substitution step, if not several steps. Recent comprehensive reviews[1] on the experimental details of organometallic ligand-substitution reactions indicate that while most information on 18-electron ML_6, ML_5, and ML_4 complexes is consistent with a dissociative mechanism proceeding via a 16-electron intermediate, there still is considerable ambiguity.[1,2] Little theoretical work has been brought to bear on this issue;[3] all of it has been confined to the computation of M-L bond dissociation energies and structural studies of 16-electron intermediates.

We have had a long-standing interest in haptotropic rearrangements,[4] wherein a ML_n unit bonded to the π system of a polyene migrates from one coordination site to another. An obviously related reaction sequence, which has a direct bearing on the ligand-substitution reaction, is the rearrangement of an ML_n unit from one coordination site to the other in a diazene complex. A description of the reactions covered in this work can be given in a generalized way for $ML_n = Cr(CO)_5$. At the ground state one nitrogen lone pair interacts with $Cr(CO)_5$ to form a Cr-N σ bond, **1**. Shifting the $Cr(CO)_5$ group to the other nitrogen

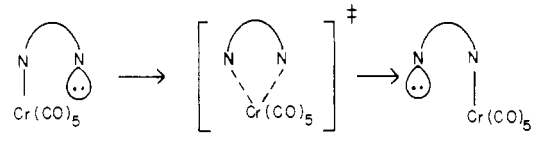

1 **2** **1'**

lone pair, **1'**, requires passage through **2**. Specific examples where this rearrangement has been experimentally investigated include $Cr(CO)_5$ complexes of azo compounds, **3**,[5] phthalazine, **4**,[6] and naphthyridine, **5**.[6] Benzocinnoline[5a,6a,7] and imidazole[8] complexes

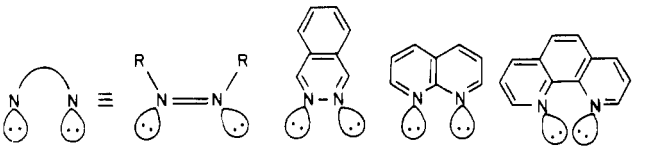

3 **4** **5** **6**

are other examples. No evidence exists for this rearrangement in $Cr(CO)_5$ complexes of 1,4-diazabutadienes,[9] and we are not aware of the synthesis of a phenanthroline complex, **6**. However, ample experimental evidence does exist for square-planar, ML_3 complexes of both ligands.[10] This type of internal ligand sub-

[†] University of Houston.
[‡] ISSECC-CNR.

(1) (a) Howell, J. A. S.; Burkinshaw, P. M. *Chem. Rev.* **1983**, *83*, 557. (b) Dobson, G. R. *Acc. Chem. Res.* **1976**, *9*, 300.
(2) See also: Basolo, F. *Inorg. Chim. Acta* **1985**, *100*, 33; **1981**, *50*, 65.
(3) For a review see: Dedieu, A. *Topics in Physical Organometallic Chemistry*; Gielen, M. F., Ed.; Freund: London, 1985; Vol 1, pp 1-141.
(4) (a) Hofmann, P.; Albright, T. A. *Angew. Chem.* **1980**, *92*, 747. (b) Albright, T. A. *J. Organomet. Chem.* **1980**, *198*, 159. (c) Albright, T. A.; Geiger, W. E.; Moraczewski, J.; Tulynathan, B. *J. Am. Chem. Soc.* **1981**, *103*, 4787. (d) Mealli, C.; Midollini, S.; Moneti, S.; Sacconi, L.; Silvestre, J.; Albright, T. A. *Ibid.* **1982**, *104*, 95. (e) Albright, T. A.; Hofmann, P.; Hoffmann, R.; Lillya, C. P.; Dobosch, P. A. *Ibid.* **1983**, *105*, 3396. (f) Silverstre, J.; Albright, T. A. *Ibid.* **1985**, *107*, 6829. (g) Karel, K. J.; Albright, T. A.; Brookhart, M. *Organometallics* **1982**, *1*, 419. (h) Silvestre, J.; Albright, T. A. *Nouv. J. Chim.* **1985**, *9*, 659.
(5) (a) Ackermann, M. N.; Willett, R. M.; Englert, M. H.; Barton, C. R.; Shewitz, D. B. *J. Organomet. Chem.* **1979**, *175*, 205. (b) Ackermann, M. N.; Shewitz, D. B.; Barton, C. R. *Ibid.* **1977**, *125*, C33. (c) Frazier, C. C., III; Kisch, H. *Inorg. Chem.* **1978**, *17*, 2736. (d) Herberhold, M.; Leonhard, K. *Angew. Chem.* **1976**, *88*, 227. (e) For isolobal benzene-$Cr(CO)_2$ complexes, see: Herberhold, M.; Leonhard, K.; Kreiter, C. G. *Chem. Ber.* **1974**, *107*, 3222.
(6) (a) Dixon, K. R.; Eadie, D. J.; Stobart, S. R. *Inorg. Chem.* **1982**, *21*, 4318. (b) Reed, T. E. Hendricker, D. G. *J. Coord. Chem.* **1972**, *2*, 83.
(7) Kooti, M.; Nixon, J. F. *J. Organomet. Chem.* **1976**, *105*, 217.
(8) (a) Hog, M. F.; Johnson, C. R.; Paden, S.; Shepherd, R. E. *Inorg. Chem.* **1983**, *22*, 2693. (b) Purcell, W. L. *Ibid.* **1983**, *22*, 1205. (c) Ellis, W. R., Jr.; Purcell, W. L. *Ibid.* **1982**, *21*, 834. (d) Balahura, R. J.; Purcell, W. L.; Victoriano, M. E.; Lieberman, M. L.; Loyola, V. M.; Fleming, W.; Fronabarger, J. W. *Ibid.* **1983**, *22*, 3602.
(9) (a) Schadt, M. J.; Lees, A. J. *Inorg. Chem.* **1986**, *25*, 672. (b) Schadt, M. J.; Gresalfi, N. J.; Lees, A. J. *Ibid.* **1985**, *24*, 2942.

0020-1669/87/1326-3158$01.50/0